SUPPLEMENTARY METHODS

Screen analysis and scoring. All plates were processed in batches at the time of screening and each batch contained at least 8 replicates containing control MCF10A cells. In the screen, each 384-well plate contains one cell line (experimental or control) treated with the normalized 90-drug library in quadruplicate (technical replicates). After proliferation data is collected, each plate is median centered to 2,000 cells/well to normalize relative proliferation rates. Plates were next filtered to those that had a minimum internal correlation across the 4 replicate wells of 0.7. In each batch, at least 2 independent plates containing control cell lines were averaged together. Each well in the experimental plate was then compared to the same well in the average control plate. Typically these values were highly correlated but in some cases there were non-linear relationships between the two plates because of differences in growth rates (i.e. one line overgrows and reaches maximum confluence for some wells). To normalize these effects, we used a sliding window based on the normalized cell number to align the median of wells in this window to the median in the comparison plate. The number of windows in this study was set to 25. This alignment enforces an overall linear relationship between experimental and control plates based on the assumption that most drugs do not have a differential effect between cell lines. Next, the set of 4 normalized replicate values in the control plate was compared to the same in the experimental plate and both the fold change in cell number and the p-value of significance of this difference in medians was calculated using a modified t-test. To avoid spurious p-values due to abnormally low variance among replicates, a minimum variance of $2x10^4$ was used for the t-test. The S-score of genetic interaction is defined by the negative $\log_{10}$ of this p-value and signed with either positive (gene drives resistance to drug) or negative (gene drives sensitivity to drug) values. Each cell line was represented by at least two biological replicate plates. For the final dataset, genetic interaction scores among biological replicates were compared and individual plates were removed if it had <0.7 correlation with other matched biological replicates. Finally, S-scores based on the biological replicates were averaged with at least 16 replicates (8 control and 8 experimental) used for final scoring. FDR was calculated based on

empirical FDR estimation (1). The entire described protocol is available in Matlab and code and raw data to recreate the dataset are published at: https://github.com/BandyopadhyayLab/chemicalgenetics.

Overlap with the Cancer Genome Project (CGP). CGP gene-drug associations were downloaded from the genomics of drug sensitivity in cancer website (www.cancerrxgene.org/downloads/, February 2013) using a p-value cutoff of 0.05 to define significant CGP gene-drug pairs (encompassing sensitivity and resistance). Comparison using the CGP was performed instead of the CCLE (2) due to lack of overlap between drugs used in our study and those in the CCLE (n=11). For data in this study, the set of gene-drug pairs were identified as those with an absolute value of S-score greater than a given cutoff. Between our dataset and the CGP there were a total of 20 genes and 40 drugs that overlapped, encompassing 800 total possible gene-drug associations. For any given cutoff, the percentage of identified gene-drug pairs that overlapped with significant CGP gene-drug pairs was determined. The significance of this overlap was determined by a hypergeometric test using the 800 (20x40) possible connections between genes and drugs shared between the two datasets as background.

Dasatinib bead proteomics. Dasatinib was conjugated to agarose beads as previously described (3). Briefly, 1.5 mg of pre-cleared cell lysate prepared in 50 mM HEPES (pH 7.5), 0.5% Triton X-100, 1 M NaCl, 1 mM EDTA, 1 mM EGTA, 1X protease inhibitor cocktail and PhosSTOP (Roche), was bound to 50 mL50 μL dasatinib-coupled beads by rotation at 4 degrees for 3 hours. Beads were washed twice with cold binding buffer, then three times with the same buffer, but with 150 mM NaCl and without Triton X-100 as described previously (4). Bound proteins were eluted with 6M Urea, trypsinized, and labeled with either TMT126 or TMT127 reagent (Pierce). Differentially labeled material from $MCF10A^{MYC}$ and $MCF10A^{PURO}$ lines were combined and peptides identified using a Thermo Velos Elite mass spectrometer. Peptides were identified using Protein Prospector. Relative TMT reporter ion intensities, which represent relative peptide abundance, were calculated for each peptide.

Antibodies. Antibodies used in this study were from the following vendors: SRC, LYN, pLYN (Tyr507), pan-Ras, GSK3β, c-KIT, PARP, BCL-2, BIM, BAX, AURKA, HA from Cell Signaling (Danvers, MA); BRAF, GAPDH, ERBB2, BCLxL, BAK from Santa Cruz Biotechnologies (Santa Cruz, CA); V5 from Invitrogen Life Technologies (Grand Island, NY); c-MYC from Epitomics (Burlingame, CA); MCL1 from Abcam (Cambridge, MA).

FACS competition assay. $MCF10A^{GFP}$ cells were combined with $MCF10A^{MYC}$ cells at a 1:1 ratio in triplicate and treated with dasatinib or DMSO for 72 hours. After treatment, cells were harvested, fixed and the proportion of cell number of GFP to MYC cells assessed by flow cytometry. Plates containing either cell line alone were used for gating controls.

siRNA knockdowns. LYN knockdowns were performed using siGENOME SMARTpool siRNAs (Thermo Scientific) targeting LYN using a pool of the following sequences: AGAUUGGAGAAGGCUUGUA, GCGACAUGAUUAAACAUUA, UGGCAUACAUCGAGCGGAA, AAGCUAAAAUAACCGGAUA. Individual siRNA sequences were performed using siON-TARGET plus siRNAs (Thermo Scientific) with the following specific sequences: siLyn #15 (GCGACAUGAUUAAACAUUA), siLyn#18 (UUACAUCUCUCCACGAAUC), siMyc #25 (AACGUUAGCUUCACCAACA), siMyc #26 (CGAUGUUGUUUCUGUGGAA). Transfection was performed using lipofectamine RNAiMAX (Invitrogen) using standard protocols.

TCGA and Clinical data analysis. Analysis was performed on 526 tumor samples used in the breast TCGA obtained from www.cbioportal.org. The PAM50 subtype breakdown of these tumors is 19% basal, 44% luminal A, 26% luminal B and 11% HER2. The I-SPY 1 TRIAL is a multi-center neoadjuvant chemotherapy breast cancer study designed to establish standards for collecting molecular and imaging data

over the course of therapy. Details of the trial have been published elsewhere (5, 6). Lowess-normalized, median-centered gene expression data at the pre-treatment time-point was available for 149 patients (GEO: GSE22226). MYC and LYN expression levels were computed as the average across probes representing these genes. Patients were dichotomized into MYC^{high} and MYC^{low} groups at the 3rd tertile; and similarly, patients with LYN expression levels in the 3rd tertile were defined as LYN^{high}. Association between recurrence free survival and MYC and LYN expression groups were visualized using Kaplan Meier curves; and significance was assessed using the log rank test.

SUPPLEMENTARY REFERENCES

1. Efron B, Tibshirani R. Empirical bayes methods and false discovery rates for microarrays. Genetic epidemiology. 2002;23:70-86.
2. Barretina J, Caponigro G, Stransky N, Venkatesan K, Margolin AA, Kim S, et al. The Cancer Cell Line Encyclopedia enables predictive modelling of anticancer drug sensitivity. Nature. 2012;483:603-7.
3. Duncan JS, Whittle MC, Nakamura K, Abell AN, Midland AA, Zawistowski JS, et al. Dynamic reprogramming of the kinome in response to targeted MEK inhibition in triple-negative breast cancer. Cell. 2012;149:307-21.
4. Oppermann FS, Gnad F, Olsen JV, Hornberger R, Greff Z, Keri G, et al. Large-scale proteomics analysis of the human kinome. Molecular & cellular proteomics : MCP. 2009;8:1751-64.
5. Esserman LJ, Berry DA, DeMichele A, Carey L, Davis SE, Buxton M, et al. Pathologic complete response predicts recurrence-free survival more effectively by cancer subset: results from the I-SPY 1 TRIAL--CALGB 150007/150012, ACRIN 6657. Journal of clinical oncology : official journal of the American Society of Clinical Oncology. 2012;30:3242-9.
6. Esserman LJ, Berry DA, Cheang MC, Yau C, Perou CM, Carey L, et al. Chemotherapy response and recurrence-free survival in neoadjuvant breast cancer depends on biomarker profiles: results from the I-SPY 1 TRIAL (CALGB 150007/150012; ACRIN 6657). Breast cancer research and treatment. 2012;132:1049-62.

SUPPLEMENTARY FIGURES

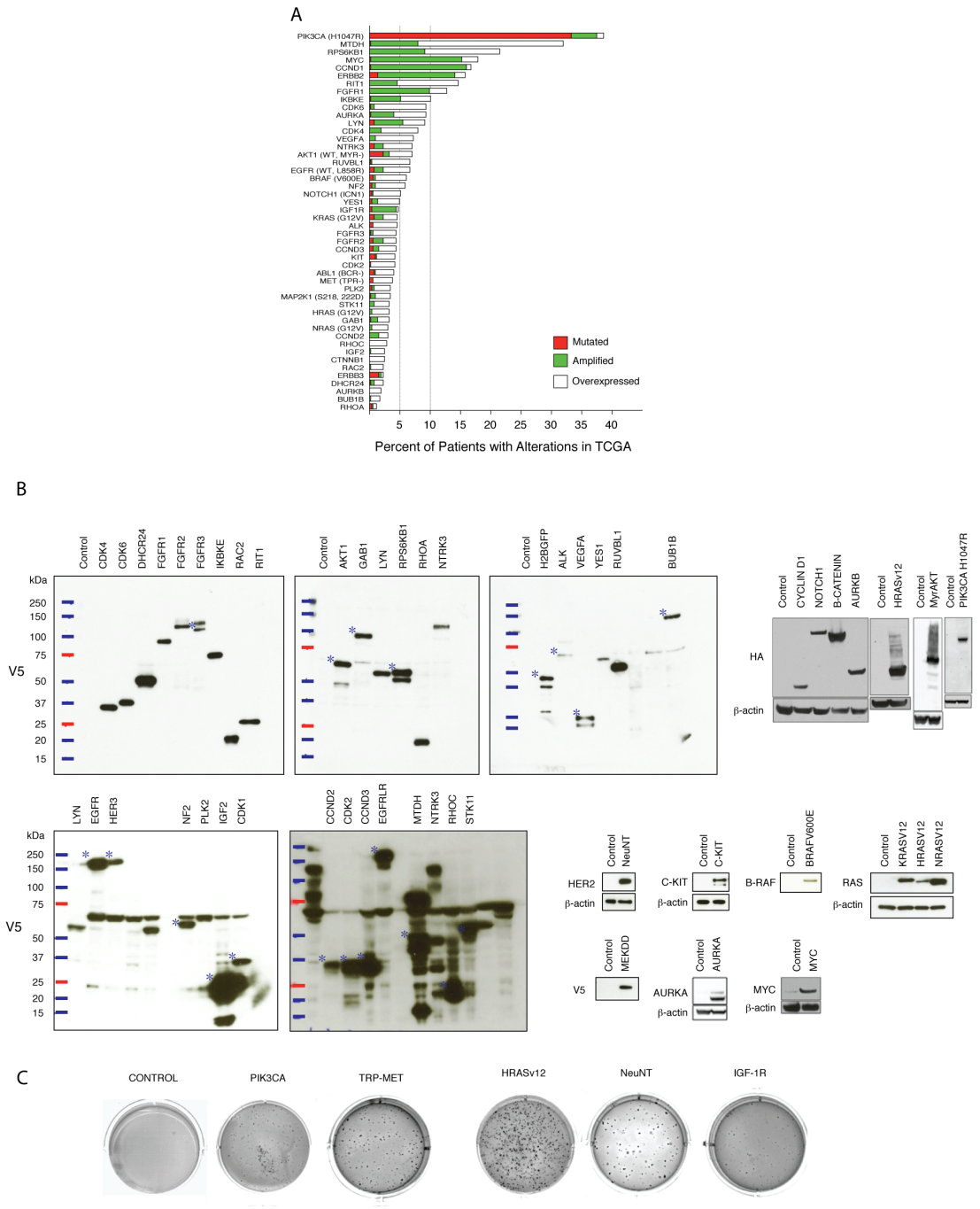

Supplementary Figure 1

Supplementary Figure 1: Distribution of gene alterations in Breast TCGA and verification of expression of MCF10A cells. (A) Genes modeled in this study sorted based on the frequency of alteration (mutation, amplification or over-expression) as indicated in the Breast TCGA. When applicable, types of mutations profiled are listed. Frequencies were obtained from the cBio portal (http://www.cbioportal.org), using Breast TCGA data (see Suppl. Methods). **(B)** Stable cell lines assayed for expression of indicated genes with epitope tags (V5, HA) or primary antibodies (HER2, KIT, BRAF, pan-RAS, AURKA, MYC). **(C)** Growth on soft agar of selected isogenic lines.

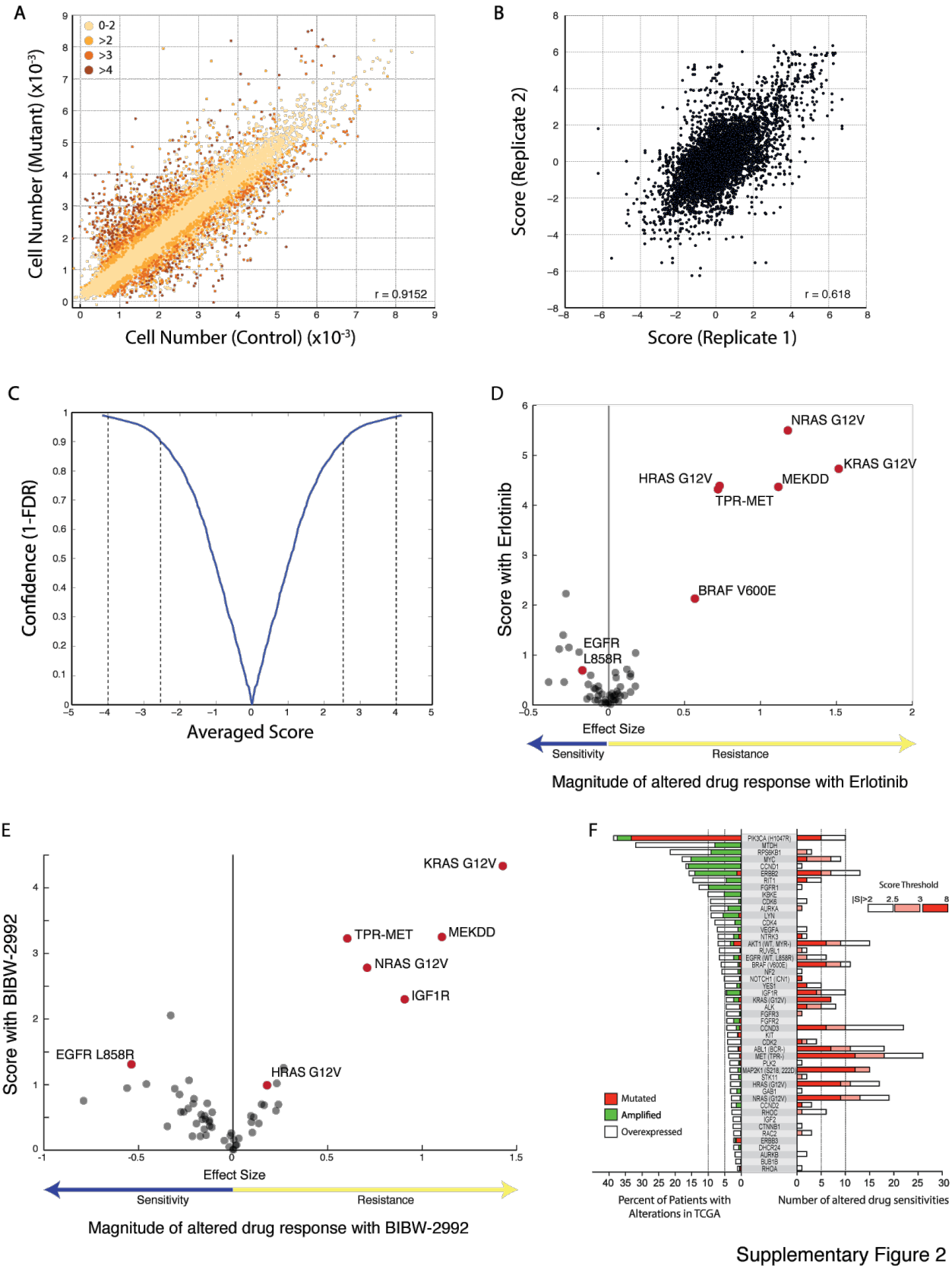

Supplementary Figure 2

Supplementary Figure 2: Analysis of the MCF10A drug screen. (A) Comparison of normalized cell number after treatment with inhibitors over all control lines versus gene-expressing lines. The chemical genetic interaction score is based on deviation from this diagonal among 4 replicates as measured by a t-test. Points reflecting various strengths of chemical-genetic interactions are

highlighted. **(B)** Scatter of chemical-genetic interaction score between all biological replicate cell lines. **(C)** False discovery rate of getting a score at least as high as the indicated value based on empirical FDR modeling based on the distribution of p-values based on a modified t-test. Vertical lines reflect 1% and 10% FDR for both positive and negative interactions. **(D-E)** Volcano plot of genes inducing resistance to the EGFR inhibitors erlotinib and BIBW-2992. Data points for the 51 cell lines in this study and their magnitude of effect and score of response is shown. Data points indicating relative sensitivity of EGFR L858R cells are shown for comparison. **(F)** Frequency of alteration compared to number of altered drug responses in this study. For each gene the number of altered drug responses (positive or negative) were counted and plotted. In cases where multiple constructs were used to model the same gene, the size of the union of their interactions was used.

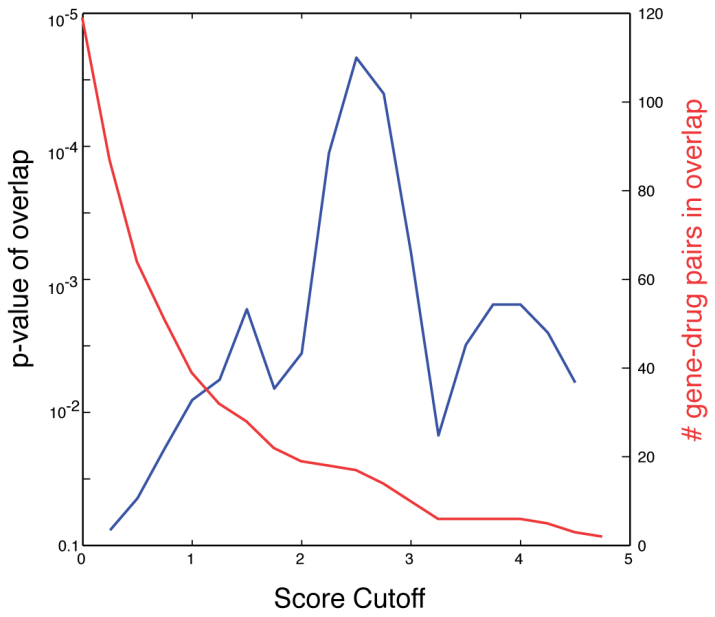

Supplementary Figure 3

Supplementary Figure 3: Significance of overlap between interactions found in this study and in the CGP. Gene drugs pairs in this study were examined using a sliding cutoff based on the absolute value of the score. The number of gene-drug pairs that overlap is in red and the significance of that overlap based on a hypergeometric test, is shown in blue.

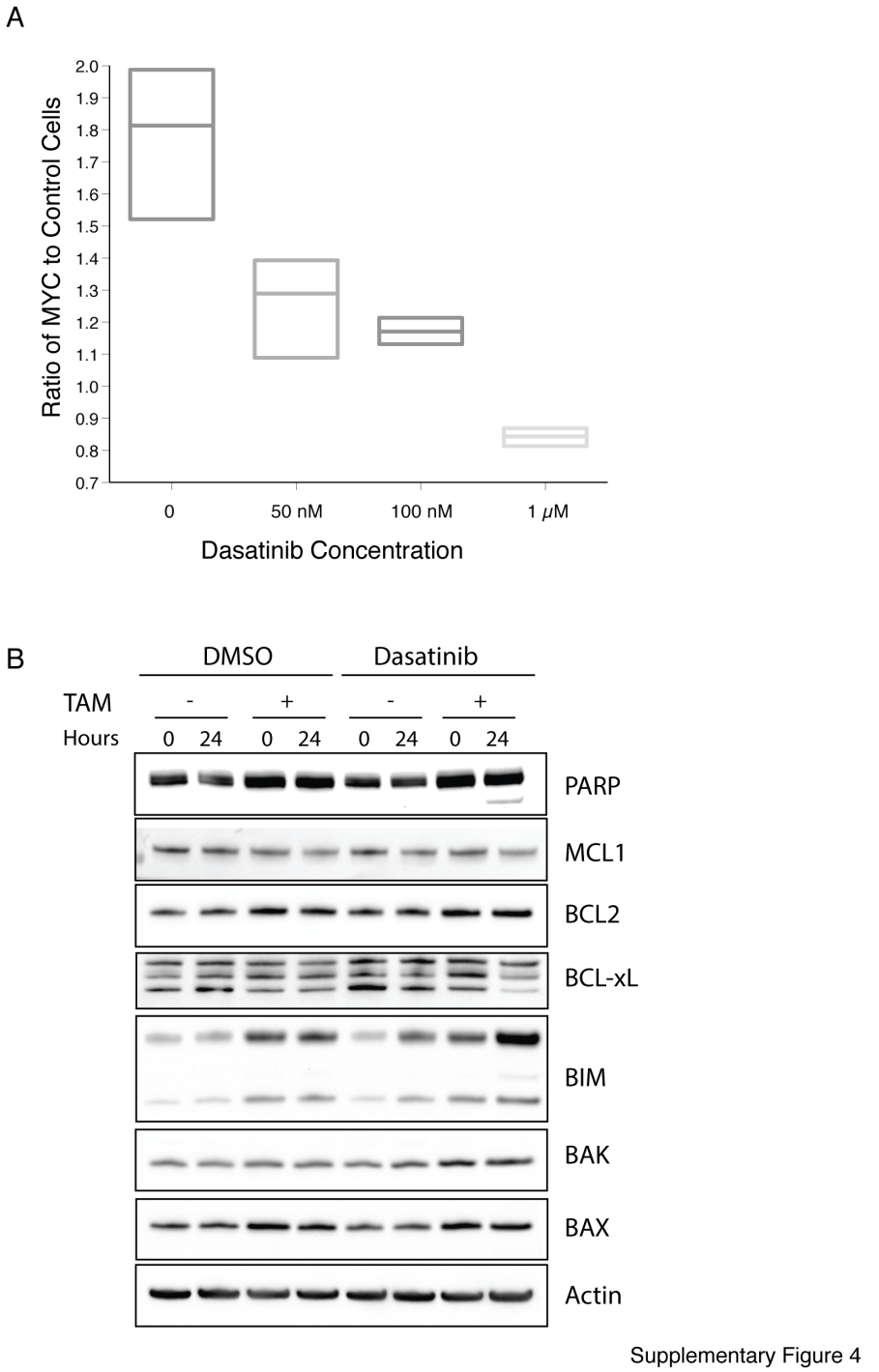

Supplementary Figure 4

Supplementary Figure 4: Response of isogenic engineered cells to dasatinib. (A) Competition assay between MCF10A^{MYC} and MCF10A^{GFP} control cells. In this assay, both cell lines were mixed at a 1:1 ratio and allowed to proliferate for 72 hours under the indicated treatment conditions. After 72 hours the proportion of each of the two cell populations were quantified using FACS. MYC cells outcompete GFP cells in untreated conditions, which is reversed when treated with dasatinib. Averages over three replicates; boxes span minimum and maximum values. **(B)** Dasatinib induces apoptosis in HMECs. Molecular markers associated with the mitochondrial apoptosis pathway after MYC activation (TAM) and treatment with 250nM dasatinib for 24 hours.

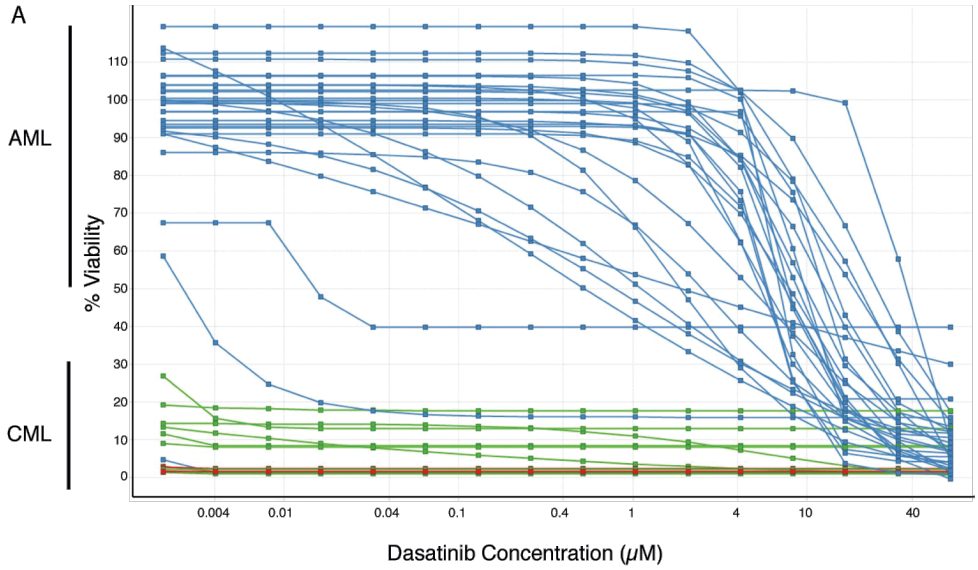

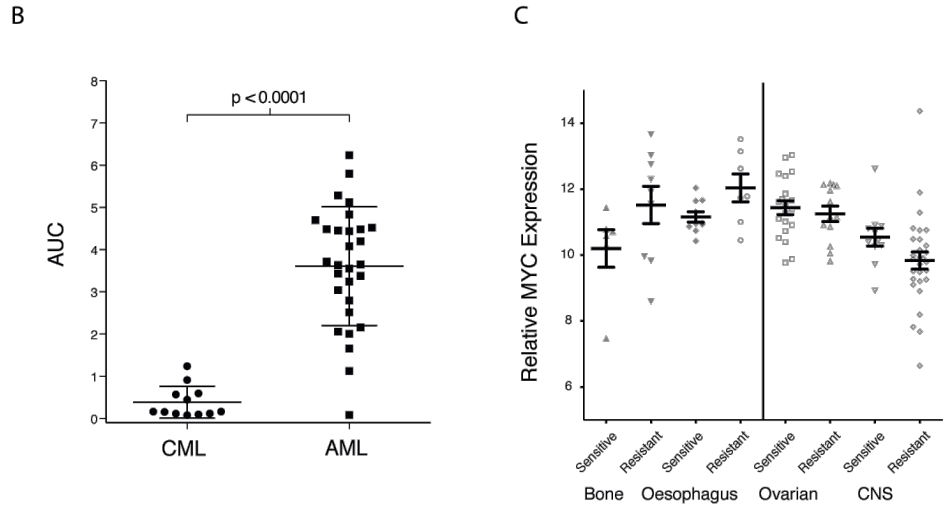

Supplementary Figure 5

Supplementary Figure 5: Dasatinib sensitivity of CML versus AML cancer cell lines. (A) Relative viability curves of CML cell lines versus AML cell lines are shown. **(B)** Comparison of AUC values for the corresponding cell lines. **(C)** Cell lines from selected tissue types stratified by dasatinib sensitivity and compared against MYC mRNA expression. Different tissue types display opposing relationships between MYC and dasatinib sensitivity.

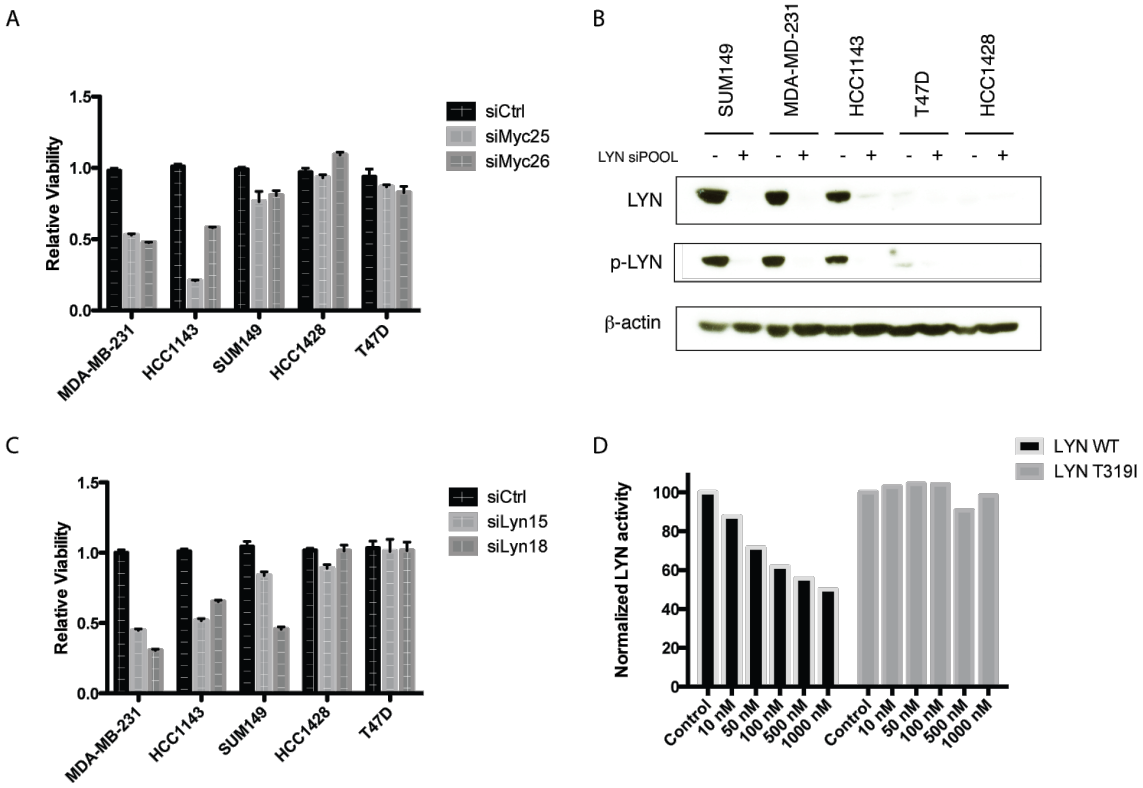

Supplementary Figure 6

Supplementary Figure 6: Verification of LYN knockown via siRNA and response of LYN T319I to dasatinib. (A) Effect of siRNA knockdown of MYC on breast cancer cell line proliferation using two independent siRNAs. **(B)** Western blot showing LYN inhibition via transfection with LYN-targeting siRNA pools in five breast cancer cell lines. **(C)** Effect of two independent LYN siRNAs on proliferation in breast cancer cell lines. **(D)** Response of MDAMB231 cells expressing wild-type LYN or LYN T319I treated with indicated doses of dasatinib though quantification of western blot. For each treatment the relative intensity of phospho-LYN (Y416) versus total-LYN bands were quantified and compared to the same ratio in DMSO control treated cells.

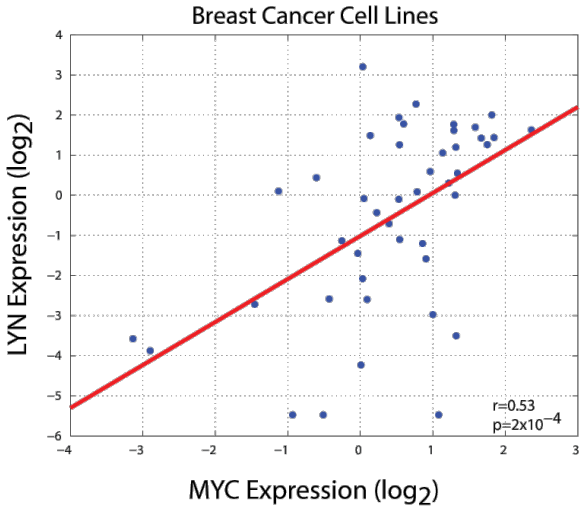

Supplementary Figure 7

Supplementary Figure 7: Co-expression of MYC and LYN in breast cancer cell lines. Expression of MYC and LYN compared across 41 breast cancer cell lines determined by RNAseq (median normalized fraction reads per kilobase mapped, FPKM). Data from (Daemen et al., 2013).

SUPPLEMENTARY TABLES

Table S1: List of constructs used to generate stable cell lines

Table S2: Drugs and their concentrations used in the isogenic drug screen

Table S3: Chemical-genetic interaction scores derived in this study

Table S4: List of 664 cancer cell lines and sensitivity to dasatinib as determined by area under the curve (AUC) in this study.

Table S5: Quantification of peptides identified bound to dasatinib by mass spectrometry.